Available online at www.sciencedirect.com
ScienceDirect
Solar Energy 83 (2009) 1370–1378
SOLAR ENERGY
www.elsevier.com/locate/solener

Robust maximum power point tracking method for photovoltaic cells: A sliding mode control approach

Chen-Chi Chu [a], Chieh-Li Chen [b,*]

[a] Aerospace Engineering and Mechanics, University of Minnesota, Minneapolis, USA
[b] Department of Aeronautics and Astronautics, National Cheng Kung University, 1 University Rd., Tainan, Taiwan

Received 30 April 2007; received in revised form 26 January 2009; accepted 2 March 2009
Available online 31 March 2009

Communicated by: Associate Editor Elias Stefanakos

Abstract

Due to nonlinear I-V characteristics of photovoltaic cells, an maximum power point tracking algorithm is adopted to maximize the output power. In this paper, an approach for peak power tracking using the sliding mode control is proposed. The proposed controller is robust to environment changes and load variations. The stability and robustness of the controller are addressed. The performance of the controller is verified through simulations and experiments. It demonstrated that the proposed approach can be implemented effectively and economically.

Keywords: Photovoltaic cells; Sliding mode control; Robustness; Maximum power point tracking

1. Introduction

Due to the rising oil price and environmental regulations, the demand of utilizing alternative power sources is increased dramatically. Alternative energy and its applications have been heavily studied for the last decade. Solar energy is a promising candidate in many applications. Among solar energy applications, the photovoltaic (PV) has received much attention with many feasible applications. However, the performance of PV depends on solar insolation, ambient temperature, and load impedance. To achieve maximum power point (MPP) output of a PV system is essential for its applications. Different approach to track the MPP has been addressed in many literatures. Among these algorithms, hill-climbing (Xiao and Dunford, 2004; Koutroulis et al., 2001; Veerachary et al., 2001) and perturbation methods (Hua and Lin, 2003; Femia et al., 2005) were commonly used due to their straightforward and low-cost implementation. These two methods share the same principle by perturbing duty cycle (or PV voltage) and observing the power output, which provides useful information for tuning duty cycle. The drawback of these methods is that, at steady state, the operation point (OP) oscillates around MPP, which propositional to perturbation size. Alternative approach to overcome this defect is called the increment conductance (IncCond) (Kuo et al., 2001; Hussein and Mota, 1995; Yu et al., 2004) method, which is based on the fact that the MPP is defined by $dP_{PV}/dV_{PV} = 0$. When $dP_{PV}/dV_{PV} > 0$ (or $dP_{PV}/dV_{PV} < 0$), then the operation point is on the left (or right) of the MPP, and should be tuned toward opposite direction, where P_{PV} denotes power output of PV and V_{PV} and I_{PV} are PV voltage and PV current, respectively. The expression of dP_{PV}/dV_{PV} can be replaced by measurable parameters $dI_{PV}/dV_{PV} + I_{PV}/V_{PV}$. However, both perturbation (or hill-climbing) and IncCond methods did not perform well during rapid changing of atmospheric conditions. Therefore, modified methods (Simoes et al., 1998; Wilamowski

* Corresponding author.
E-mail address: chiehli@mail.ncku.edu.tw (C.-L. Chen).

0038-092X/$ - see front matter © 2009 Elsevier Ltd. All rights reserved.
doi:10.1016/j.solener.2009.03.005

Nomenclature

V_{PV}	PV voltage	C	Capacitance
I_{PV}	PV current	L	Inductance
P_{PV}	PV generate Power	R_L	Load resistance
R_{PV}	V_{PV}/I_{PV}	δ	Duty ratio
V_{OC}	PV open-circuit voltage	i_L	Inductor current ($= I_{PV}$)
I_{SC}	PV short-circuit current	V_o	Output voltage
V_{mpp}	Maximum power output voltage	V	Lyapunov function
I_{mpp}	Maximum power output current	σ	Sliding surface

and Li, 2002; Hiyama et al., 1995; Noguchi et al., 2002) have also been proposed to improve tracking performance.

The algorithms mentioned above are sharing the same idea of "searching for MPP". Since PV exhibits nonlinear I-V characteristics, solutions of MPP are difficult to be determined analytically. Another approach called proportional open-circuit voltage (or short-circuit current) is addressed in Chu and Chen (2008), Duru (2006), which assumed that voltage (V_{mpp}) and current (I_{mpp}) of MPP is proportion to PV open-circuit voltage (V_{oc}) and short-circuit current (I_{sc}), respectively. However, the estimated V_{mpp} is only an approximation of true V_{mpp} and the proportional constant will change if the PV module ages, in other words, the performance degraded with time.

Variable structure control approach for PV conversion system was proposed and evaluated by numerical study in Battista and Mantz (2002). Further study was also proposed in Fossas and Biel (1996), Tan et al. (2004), Kim (2007), however, these approaches required reference current for control law synthesis and may lead to a lack of robustness to operation conditions. By deliberately defining the sliding surface a robust approach was proposed in this paper. This paper is organized as follows: In Section 2, PV characteristic is described. The system model of the proposed sliding control approach MPPT is discussed in Section 3. The sliding approach is given in Section 4. Simulation and experimental results are given in Sections 5 and 6, respectively. Conclusion is addressed in the last section.

2. PV characteristic

PV array is a p-n junction semiconductor, which converts light into electricity. When the incoming solar energy exceeds the band-gap energy of the module, photons are absorbed by materials to generate electricity. The equivalent-circuit model of PV is shown in Fig. 1. In this model, it consists of a light-generated source, diode, series and parallel resistances. The mathematical expression of the equivalent model can be written as (1)–(3). Where R_s is relatively small and R_{sh} is relatively large, which are neglected in the equation in order to simplify the simulation.

$$I = I_{ph} - I_d\left[\exp\left(\frac{q}{k_b TA}V\right) - 1\right] \quad (1)$$

$$I_{ph} = S[I_{scr} + k_i(T - T_r)] \quad (2)$$

$$I_d = I_{rr}\left[\frac{T}{T_r}\right]^3 \exp\left(\frac{qE_g}{kQA}\left[\frac{1}{T_r} - \frac{1}{T}\right]\right) \quad (3)$$

where

I, V output current, voltage (A, V).
T cell temperature (K).
S solar irradiance (W/m^2).
I_{ph} light-generated current.
I_d PV saturation current.
I_{rr} saturation current at T_r.
I_{scr} short-circuit current at reference condition.
T_r reference temperature.
K_i short-circuit temperature coefficient.
q charge of an electron.
k_b Boltzmann's constant.
E_g band-gap energy of the material.
Q total electron charge.
A ideality factor.

The PV characteristic is plotted in Fig. 2 under different irradiance levels, and PV characteristic under different temperature is plotted in Fig. 3. As illustrated in the figures, the open-circuit voltage (V_{oc}) is dominated by temperature, and solar irradiance has preeminent influence on short-

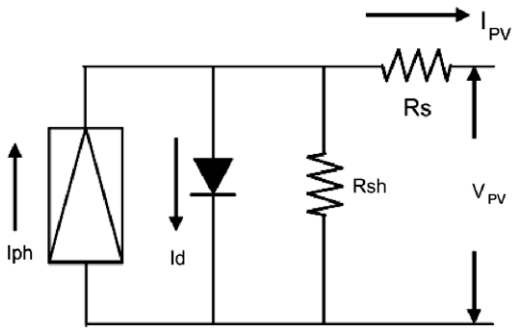

Fig. 1. Equivalent circuit model of PV.

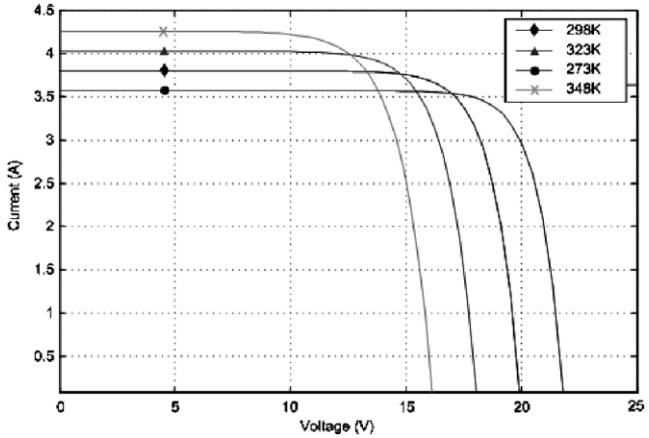

Fig. 2. PV characteristic under different temperature (irradiance = 1000 W/m^2).

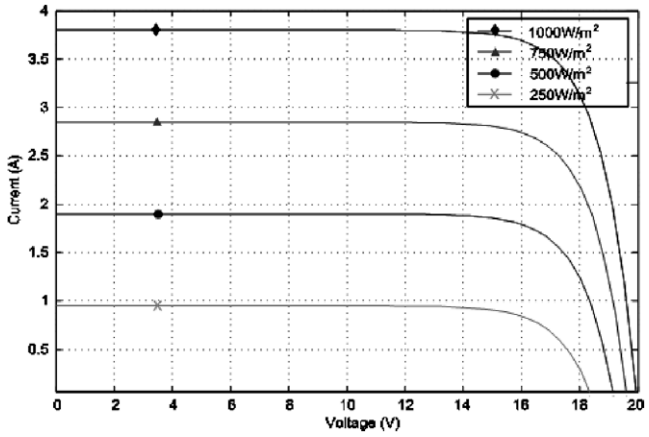

Fig. 3. PV characteristic under different irradiance levels (temperature = 273 K).

circuit current (I_{sc}). We can conclude that high temperature and low solar irradiance will reduce the power conversion capability.

3. MPPT system modeling

Consider a boost type converter connected to a PV module with a resistive load as illustrated in Fig. 4.

The system can be written in two sets of state equation depends on the position of switch S. If the switch is in position $S = 0$, the differential equation can be written as:

$$\dot{i}_{L_1} = \frac{V_{PV}(i_L)}{L} - \frac{V_o}{L} \tag{4a}$$

$$\dot{V}_{o_1} = \frac{i_L}{C} - \frac{V_o}{CR_L} \tag{4b}$$

The differential equation can be expressed as (5a) and (5b) if the switch is in position $S = 1$.

$$\dot{i}_{L_2} = \frac{V_{PV}(i_L)}{L} \tag{5a}$$

$$\dot{V}_{o_2} = -\frac{V_o}{CR_L} \tag{5b}$$

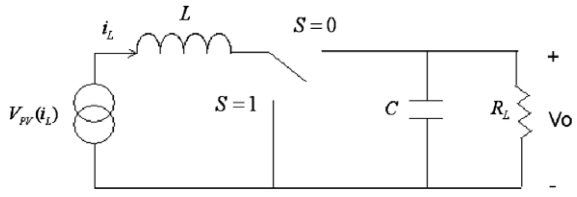

Fig. 4. MPPT system schematic.

By utilizing State Space Averaging method (Erickson and Maksimovic, 2001), Eqs. (4) and (5) can be combined into one set of state equation to represent the dynamic of the system. Base on the idea of Pulse-Width Modulation (PWM), the ratio of the switch in position 1 in a period is defined as duty ratio. Two distinct equation sets are weighted by the duty ratio and superimposed:

$$\dot{\mathbf{X}} = (1-\delta)\dot{\mathbf{X}}_1 + \delta\dot{\mathbf{X}}_2 \tag{6}$$

where $\dot{\mathbf{X}}_1 = [\dot{i}_{L_1} \quad \dot{V}_{o_1}]^T$, $\dot{\mathbf{X}}_2 = [\dot{i}_{L_2} \quad \dot{V}_{o_2}]^T$, and $\delta \in [0 \quad 1]$ is the duty ratio. Hence the dynamic equation of the system can be described by

$$\dot{i}_L = \frac{V_{PV}(i_L)}{L} - \frac{V_o}{L} + \frac{V_o}{L}\delta \tag{7a}$$

$$\dot{V}_o = \frac{i_L}{C} - \frac{V_o}{CR_L} - \frac{i_L}{C}\delta \tag{7b}$$

where C is the capacity, L is the inductance, R_L is the resistive load, $\delta \in [0 \quad 1]$ is the duty ratio, which is also the control input. V_o is the output voltage and i_L is the inductor current. Note the equivalent series resistance (ESR) of the inductor and wiring resistance are neglected in the case, so i_L is assumed to be equal to the PV current (I_{PV}). Eq. (7) can be written in general form of the nonlinear time invariant system.

$$\dot{\mathbf{X}} = f(\mathbf{X}) + g(\mathbf{X})\delta \tag{8}$$

4. Sliding mode control approach for MPPT

A typical sliding mode control has two modes of operation. One is called the approaching mode, where the system state converges to a pre-defined manifold named sliding function in finite time. The other mode is called the sliding mode, where the system state is confined on the sliding surface and is driven to the origin. In this study, we introduce the concept of the approaching control approach. By selecting the sliding surface as $\partial P_{PV}/\partial I_{PV} = 0$, it is guaranteed that the system state will hit the surface and produce maximum power output persistently.

$$\frac{\partial P_{PV}}{\partial I_{PV}} = \frac{\partial I_{PV}^2 R_{PV}}{\partial I_{PV}} = I_{PV}\left(2R_{PV} + I_{PV}\frac{\partial R_{PV}}{\partial I_{PV}}\right) = 0 \tag{9}$$

where $R_{PV} = V_{PV}/I_{PV}$ is the equivalent load connect to the PV, and I_{PV} is the PV current, which is equal to i_L in this case. The non-trivial solution of (9) is $2R_{PV} + I_{PV} \cdot \partial R_{PV}/\partial I_{PV} = 0$. Hence, the sliding surface is defined as:

$$\sigma \underline{\underline{\Delta}} 2R_{PV} + i_L \frac{\partial R_{PV}}{\partial i_L} \tag{10}$$

Based on the observation of duty cycle versus operation region as depicted in Fig. 5, the duty cycle output control can be chosen as:

$$\delta_{update} = \begin{cases} \delta + \Delta\delta \text{ for } & \sigma > 0 \\ \delta - \Delta\delta \text{ for } & \sigma < 0 \end{cases}$$

In order to get the equivalent control (δ_{eq}) suggested by Slotine and Li (2005), the equivalent control is determined from the following condition:

$$\dot{\sigma} = \left[\frac{\partial \sigma}{\partial \mathbf{X}}\right]^T \dot{\mathbf{X}} = \left[\frac{\partial \sigma}{\partial \mathbf{X}}\right]^T (f(\mathbf{X}) + g(\mathbf{X})\delta_{eq}) = 0 \tag{11}$$

The equivalent control is then derived:

$$\delta_{eq} = -\frac{\left[\frac{\partial \sigma}{\partial \mathbf{X}}\right]^T f(\mathbf{X})}{\left[\frac{\partial \sigma}{\partial \mathbf{X}}\right]^T g(\mathbf{X})} = 1 - \frac{V_{PV}(i_L)}{V_o} \tag{12}$$

since the range of duty cycle must lies in $0 \leqslant \delta_{eq} \leqslant 1$, the real control signal is proposed as:

$$\delta = \begin{cases} 1 & \delta_{eq} + k\sigma \geqslant 1 \\ \delta_{eq} + k\sigma, \quad \text{for} & 0 < \delta_{eq} + k\sigma < 1 \\ 0 & \delta_{eq} + k\sigma \leqslant 0 \end{cases} \tag{13}$$

where the control saturate if $\delta_{eq} + k\sigma$ is out of range, and k is a positive scaling constant. The proposed control is comprised with δ_{eq} and $k\sigma$, where δ_{eq} is the required effort for $\dot{\sigma} = 0$ and $k\sigma$ can be considered as the effort to track the MPP. The existence of the approaching mode of the proposed sliding function σ is provided.

A Lyapunov function is defined as:

$$V := \frac{1}{2}\sigma^2 \tag{14}$$

The time derivative of σ can be written as:

$$\begin{aligned} \dot{\sigma} &= \left[\frac{\partial \sigma}{\partial \mathbf{X}}\right]^T \dot{\mathbf{X}} \\ &= \left(3\frac{\partial R_{PV}}{\partial i_L} + i_L \frac{\partial^2 R_{PV}}{\partial i_L^2}\right)\left(-\frac{V_o}{L}(1-\delta) + \frac{V_{PV}(i_L)}{L}\right) \end{aligned} \tag{15}$$

Replacing R_{PV} by the definition of $R_{PV} = V_{PV}/I_{PV}$

$$\frac{\partial R_{PV}}{\partial i_L} = \frac{\partial}{\partial i_L}\left[\frac{V_{PV}}{i_L}\right] = \frac{1}{i_L}\frac{\partial V_{PV}}{\partial i_L} - \frac{V_{PV}}{i_L^2} \tag{16}$$

$$\frac{\partial^2 R_{PV}}{\partial i_L^2} = \frac{1}{i_L}\frac{\partial^2 V_{PV}}{\partial i_L^2} - \frac{2}{i_L^2}\frac{\partial V_{PV}}{\partial i_L} + \frac{2V_{PV}}{i_L^3} \tag{17}$$

By (4), the PV voltage (V_{PV}) can be rewritten as function of PV current (I_{PV})

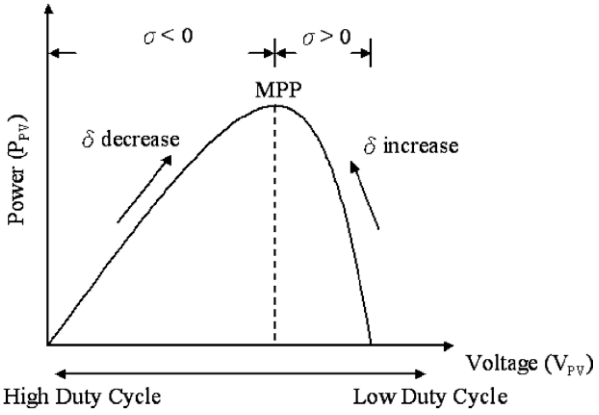

Fig. 5. Duty cycle versus operation region.

$$V_{PV} = \frac{K_b T A}{q} \ln\left(\frac{I_{ph} + I_d - I_{PV}}{I_d}\right) \tag{18}$$

$$\frac{\partial V_{PV}}{\partial I_{PV}} = -\frac{K_b T A}{q}\frac{I_0}{I_{ph} + I_0 - I_{PV}} < 0 \tag{19}$$

$$\frac{\partial^2 V_{PV}}{\partial I_{PV}^2} = -\frac{K_b T A}{q}\frac{I_0}{(I_{ph} + I_0 - I_{PV})^2} < 0 \tag{20}$$

Substitute (16) and (17) into (15) yield

$$\begin{aligned} \left[\frac{\partial \sigma}{\partial \mathbf{X}}\right]^T &= 3\frac{\partial R_{PV}}{\partial i_L} + i_L \frac{\partial^2 R_{PV}}{\partial i_L^2} \\ &= \frac{1}{i_L}\frac{\partial V_{PV}}{\partial i_L} - \frac{V_{PV}}{i_L^2} + \frac{\partial^2 V_{PV}}{\partial i_L^2} < 0 \end{aligned} \tag{21}$$

According to the result of (19) and (20) and $V_{PV}/i_L^2 > 0$, the sign of (21) is negative definite.

The achievability of $\sigma = 0$ will be obtained by $\sigma\dot{\sigma} < 0$ for all δ discussed as follows.

For $0 < \delta < 1$,

$$\begin{aligned} \dot{X} &= -\frac{V_o}{L}(1-\delta) + \frac{V_{PV}(i_L)}{L} \\ &= -\frac{V_o}{L}(1 - \delta_{eq} - k\sigma) + \frac{V_{PV}(i_L)}{L} \\ &= -\frac{V_o}{L}\left(1 - \left(1 - \frac{V_{PV}(i_L)}{V_o}\right) - k\sigma\right) + \frac{V_{PV}(i_L)}{L} \\ &= \frac{V_o}{L}k\sigma \end{aligned} \tag{22}$$

Based on the result of (21) and (22), $\dot{\sigma}$ always has inverse sign of σ. Therefore, $\dot{\sigma}\sigma < 0$ is obtained for $0 < \delta < 1$.

For $\delta = 1$,

$$\dot{X} = \frac{V_{PV}(i_L)}{L} > 0 \tag{23}$$

By (21) and (23), $\dot{\sigma} < 0$. With $\delta = 1$, two cases should be examined for the fulfillment of $\dot{\sigma}\sigma < 0$.

(1) $\delta_{eq} = 1$.
If $\delta_{eq} = 1$, it implies $V_{pv}(i_L) = 0$ which means the system is operating at the left-hand corner of

Fig. 5, and σ is negative for this case. Therefore, $\delta_{eq} + k\sigma$ will be less than 1, which contradicts to the assumption of $\delta = 1$.

(2) $\delta_{eq} < 1$ and $\delta_{eq} + k\sigma \geqslant 1$.
If $\delta_{eq} < 1$, but$\delta_{eq} + k\sigma \geqslant 1$, it implies $\sigma > 0$ and $\dot{\sigma}\sigma < 0$.

It concludes that $\dot{\sigma}\sigma < 0$ for $\delta = 1$.

For $\delta = 0$,

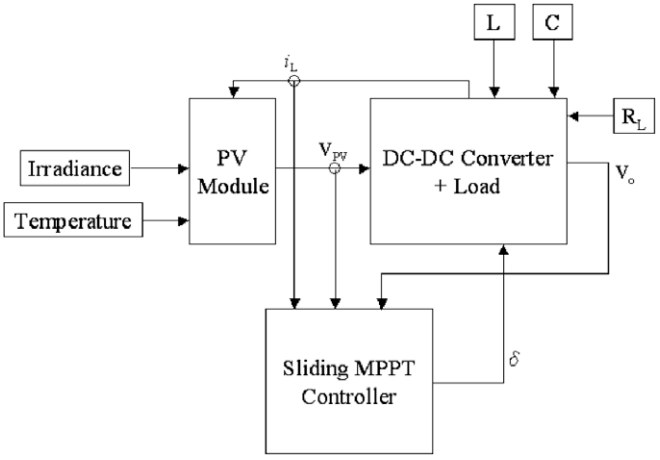

Fig. 6. MPPT system block diagram.

Table 1
System specification.

Parameters	Value	Parameters	Value
I_{rr}	5.981×10^{-8} (A)	q	1.6×10^{-19} (C)
I_{scr}	3.81 (A)	k_b	1.38×10^{-23} (J/K)
T_r	298 (K)	E_g	1.12 (V)
K_i	0.0024	A	1.2
L	1.5 (mH)	C	500 (uF)
k	0.001		

$$\dot{X} = -\frac{V_o}{L} + \frac{V_{PV}(i_L)}{L} < 0 \tag{24}$$

In this case, the output voltage (V_o) is higher than the input voltage (V_{pv}). From (21) and (24), it results that $\dot{\sigma} > 0$. Two cases for $\delta = 0$ are examined as follows.

(1) $\delta_{eq} = 0$.
$\delta_{eq} = 0$ implies $V_{PV}(i_L) = V_O$, which corresponding to the situation that the PV module is directly connected to the load and operates in the region $\sigma > 0$. As the result $\delta > 0$ and it contradicts to the assumption of $\delta = 0$.

(2) $\delta_{eq} > 0$ and $\delta_{eq} + k\sigma \leqslant 0$
In this case, $\sigma < 0$ is obtained and $\dot{\sigma}\sigma < 0$.

It concludes that $\dot{\sigma}\sigma < 0$ for $\delta = 0$.

From the discussion above, the existence of the MPP state $\sigma = 0$ can be guaranteed using the proposed control law (13). One thing worth to notice, to avoid the controller always saturates on the states $\delta = 0$ or $\delta = 1$ without hitting the range of $0 < \delta < 1$, the scaling constant k should not be selected to large (e.g. $k \leqslant 1/|\sigma|_{max}$), where $|\sigma|_{max}$ is the maximum absolute value of sliding surface σ. $|\sigma|_{max}$ presents when $\delta_{eq} = 0$,

$$|\sigma|_{max} = \sigma|_{\delta_{eq}=0} = -\frac{k_b T A}{q} \frac{I_0}{I_{ph} + I_0 - I_{PV}} + R_L \approx R_L \tag{25}$$

Hence $k \leqq 1/R_L$ can avoid the situation.

5. Simulation results

The PV model, boost type converter model, and proposed MPPT approach are implemented in Matlab/Simulink as illustrated in Fig. 6. In the study, KC-60 PV module manufactured by Kyocera Solar Inc. has been

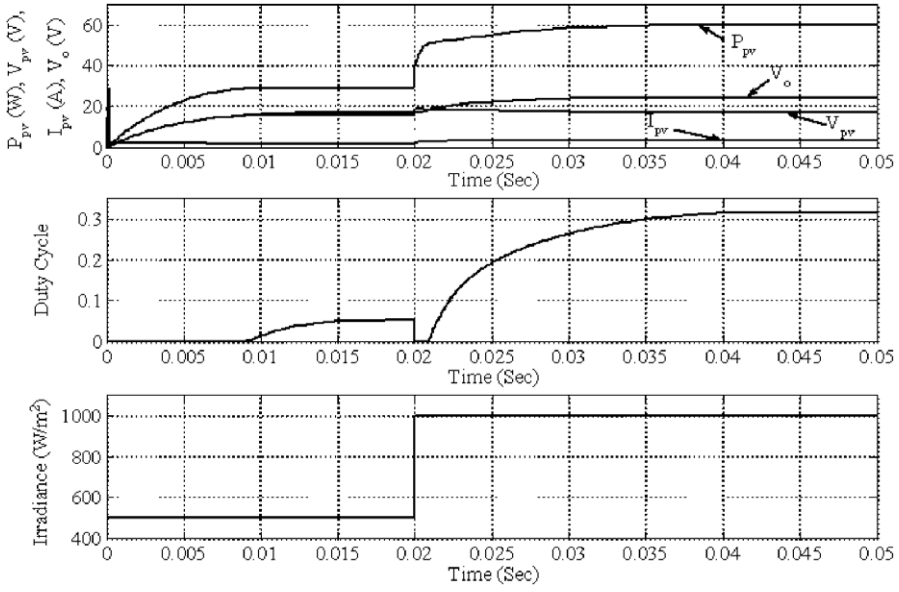

Fig. 7. Simulation with step irradiance change (500 → 1000 W/m^2, temperature = 300 K, $R_L = 10\ \Omega$).

selected as PV power source, and the parameter of the components are chosen to deliver maximum 60 W of power generated by KC-60. The specification of the system is tabulated in Table 1. The proposed MPPT is evaluated from three aspects: robustness to irradiance, temperature, and load. In each figures, two different values of irradiance, temperature or load are presented for comparison in order to show the robustness.

Fig. 7 illustrates the tracking result with step irradiance input ($500 \rightarrow 1000\ W/m^2$) under the same temperature and load. The system reaches steady state of both irradiance levels within the order of milliseconds, which is much faster compare to the other MPPT tracking techniques. Figs. 8 and 9 depict respectively the system response under rapid temperature change and load variation. In Fig. 8, sliding control MPPT is tested under sudden change of temperature from 273 to 323 K, which is quite normal for space application. And Fig. 9 simulates the transit of a lightly loaded system to a heavily loaded system (from 100 to 10 Ω). For all the results above, the sliding mode approach is able to maintain the output at optimum point and robust to the variation of the external conditions. Furthermore, it can almost reach the theoretical maximum power of known irradiance and temperature. The theoretical maximum powers of simulated condition are tabulated in Table 2.

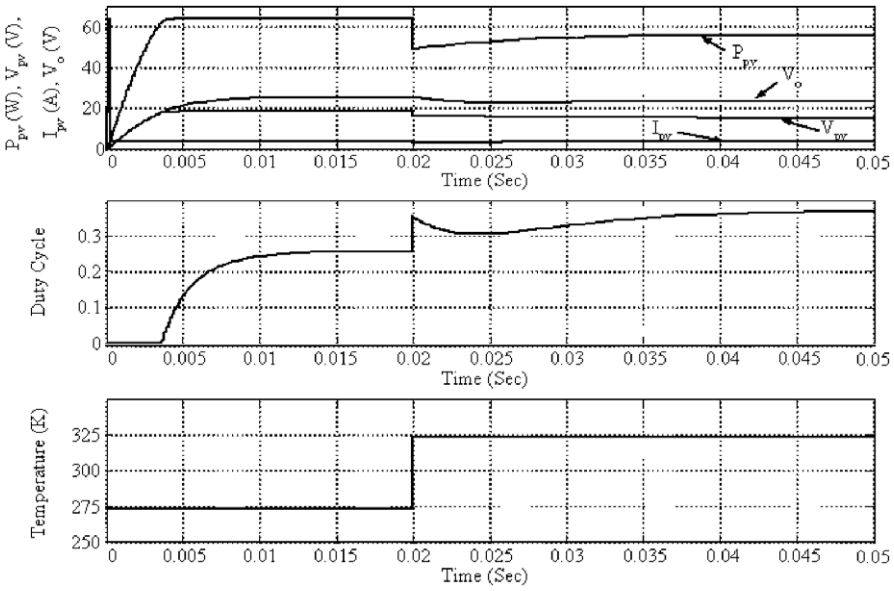

Fig. 8. Simulation with step temperature change (273 → 323 K, $I_{rr} = 1000\ W/m^2$, $R_L = 10\ \Omega$).

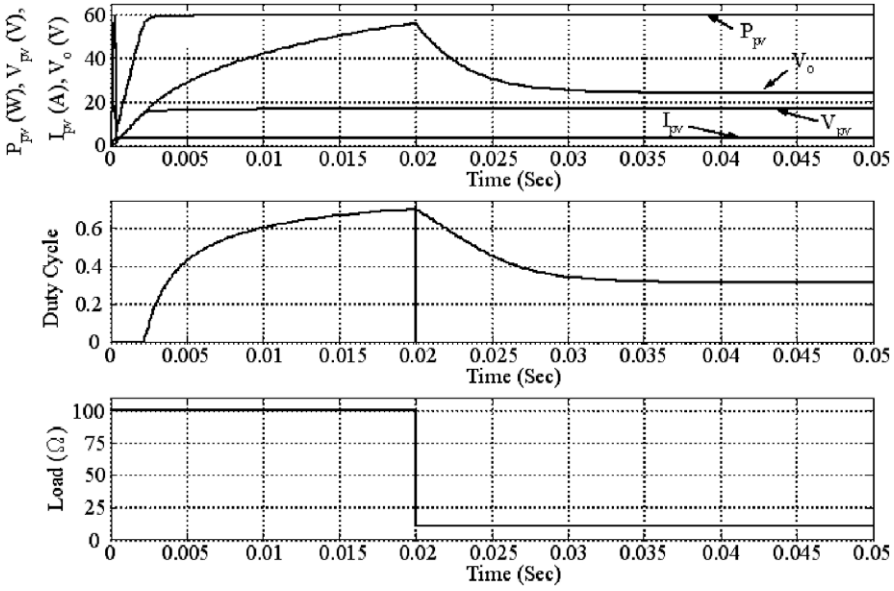

Fig. 9. Simulation with step load change (100 → 10 Ω, $I_{rr} = 1000\ W/m^2$, temperature = 300 K).

Table 2
Theoretical maximum power.

Irradiance (W/m^2)	Temperature (K)	Maximum power (W)
500	300	28.51
1000	300	59.78
1000	273	63.70
1000	323	55.71

6. Experiment results

To verify the performance of the proposed sliding mode MPPT, the experiment configuration is set up as shown in Fig. 10, where a boost type converter is adopted. The PWM signal is generated by TL494 (Texas Instruments), which is operated at 20 KHz. The duty cycle control signal is fed by a voltage level ranges from 0.9 to 3.6 V to generate duty cycle varies from approximate 92–0%. The input and output of analog signals are processed by a USB DAQ device (USB-6009) manufactured by National Instruments. Current information is obtained by the voltage drop across a 5 mΩ resister. The voltage drop is input to an INA with 500× amplification, then pass to DAQ for computation.

The experiment is conducted under the irradiance 830 W/m^2, and the PV module temperature is of 33 °C (306 K). A 50 Ω resistor is connected as load. The resulting waveform of the proposed controller is illustrated in Fig. 11. The PV power, PV voltage, and PV current are provided in associated with duty cycle. The power variation is mainly caused by low sampling rate and can be

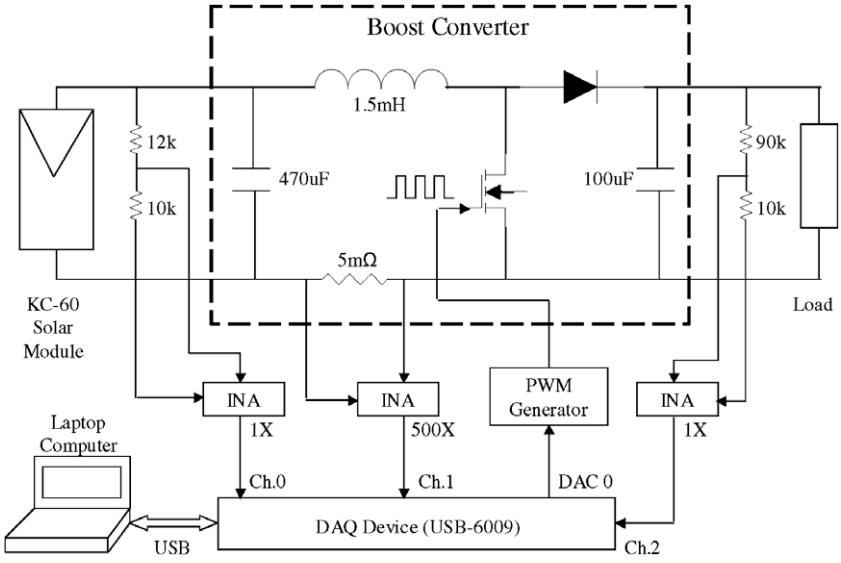

Fig. 10. Experiment configuration.

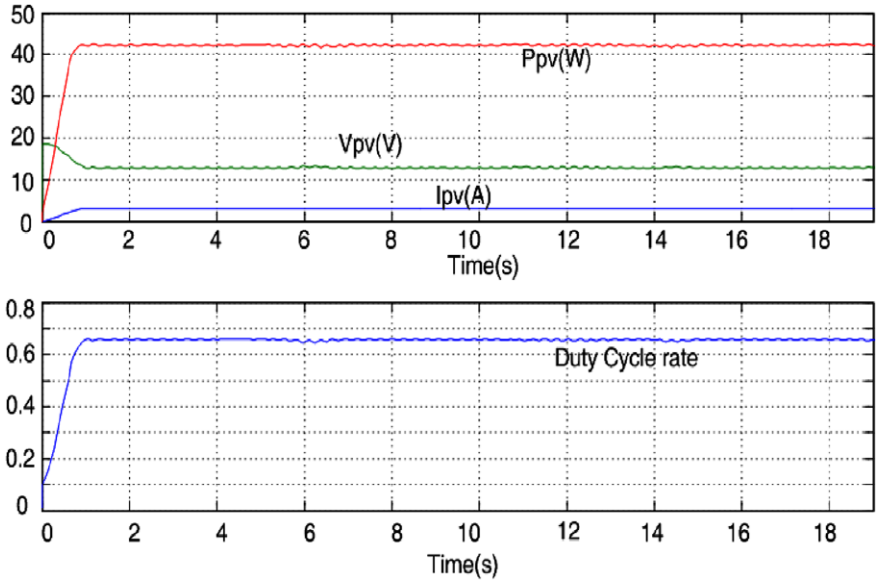

Fig. 11. Experiment results.

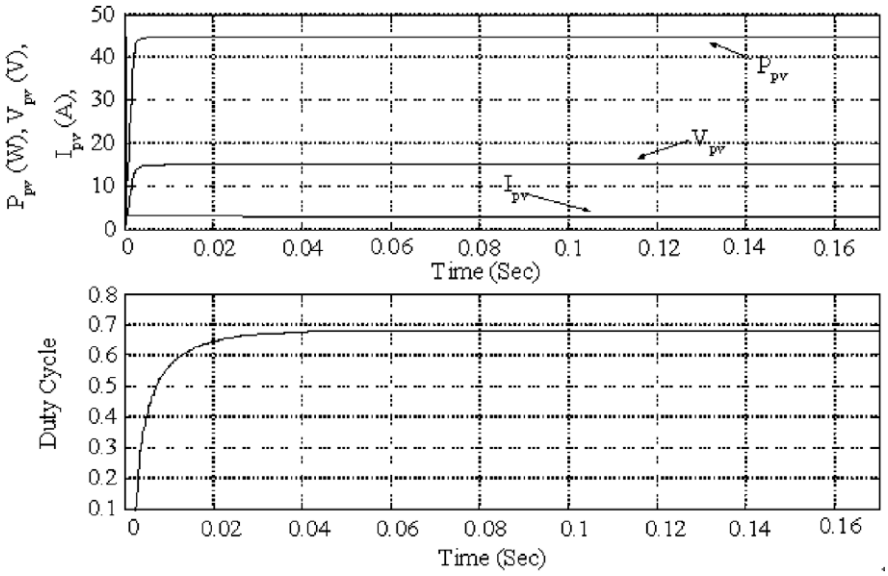

Fig. 12. Simulation results.

improved with high performance DAQ interface. The maximum power output obtained by numerical simulation under the same operation condition is shown Fig. 12, which conformed to the experimental result.

7. Conclusions

A switched system model was introduced to design maximum peak power tracking controller for PV cells based on the sliding mode control approach, where $\frac{\partial P_{PV}}{\partial I_{PV}} = 0$ is used as the sliding function. The stability of the control system was also addressed. Different to the approaches (Duru, 2006; Battista and Mantz, 2002; Fossas and Biel, 1996; Tan et al., 2004), no desired reference was required in the proposed method and it is robust to operation conditions and PV cells' parameter changes. Numerical results were provided and validated by experimental studies. The resulting performance can further be improved using high performance DAQ device. The proposed approach provides a feasible approach to manage PV power systems.

Acknowledgements

The work was supported by the the Ministry of Economic Affairs (95-EC-17-A- 05-S1-0014) and National Science Council, (NSC94-2221-E006-276), Taiwan.

References

Battista, H. De, Mantz, R.J., 2002. Variable structure control of a photovoltaic energy converter. IEE Proc. Control Theor. Appl. 149, 303–310.

Chu, C.C., Chen, C.L., 2008. A variable step maximum power point tracking for photovoltaic power system. J. Chin. Soc. Mech. Eng. 29 (3), 225–231.

Duru, H.T., 2006. A maximum power tracking algorithm based on Impp = f(Pmax) function for matching passive and active loads to a photovoltaic generator. Sol. Energy 80, 812–822.

Erickson, R.W., Maksimovic, D., 2001. Fundamentals of Power Electronics. Kluwer Academic Publishers.

Femia, N., Petrone, G., Spagnuolo, G., Vitelli, M., 2005. Optimization of perturb and observe maximum power point tracking method. IEEE Trans. Power Electron. 20, 963–973.

Fossas, E., Biel, D., 1996. A sliding mode approach to robust generation on dc-to-dc nonlinear converters. In: IEEE International Workshop on Variable Structure Systems, December 1996, pp. 67–71.

Hiyama, T., Kouzuma, S., Imakubo, T., 1995. Identification of optimal operating point of PV modules using neural network for real time maximum power tracking control. IEEE Trans. Energy Conver. 10, 360–367.

Hua, C., Lin, J., 2003. An on-line MPPT algorithm for rapidly changing illuminations of solar arrays. Renew. Energy 28, 1129–1142.

Hussein, K.H., Mota, I., 1995. Maximum photovoltaic power tracking: an algorithm for rapidly changing atmospheric conditions. IEE Proc. Generation Transm. Distrib. 1, 59–64.

Kim, I.-S., 2007. Robust maximum power point tracker using sliding mode controller for the three-phase grid-connected photovoltaic system. Sol. Energy 81, 405–414.

Koutroulis, E., Kalaitzakis, K., Voulgaris, N.C., 2001. Development of a microcontroller-based. Photovoltaic maximum power point tracking control system. IEEE Trans. Power Electron. 16, 46–54.

Kuo, Y.C., Liang, T.J., Chen, J.F., 2001. Novel maximum-power-point tracking controller for photovoltaic energy conversion system. IEEE Trans. Ind. Electron. 48, 594–601.

Noguchi, T., Togashi, S., Nakamoto, R., 2002. Short-current pulse-based maximum-power-point tracking method for multiple photovoltaic-and-converter module system. IEEE Trans. Ind. Electron. 49, 217–223.

Simoes, M.G., Franceschetti, N.N., Friedhofer, M., 1998. A fuzzy logic based photovoltaic peak power tracking control. In: Proceedings of IEEE International Symp. on Ind. Electron. (ISIE'98), Pretoria, South Africa, pp. 300–305.

Slotine, J.-J.E., Li, W., 2005. Applied Nonlinear Control, third ed. Addison Wesley.

Tan, S., Lai, Y.M., Tse, C.K., Cheung, M.K.H., 2004. An adaptive sliding mode controller for buck converter in continuous conduction mode. In: Proceedings of Applied Power Electronics Conference and Exposition (APEC'04), Anaheim, California, pp. 1395–1400.

Veerachary, M., Senjyu, T., Uezato, K., 2001. Maximum power point tracking control of IDB converter supplied PV system. IEE Proc. Electron. Power Appl. 148, 494–502.

Wilamowski, B.M., Li, X., 2002. Fuzzy system based maximum power point tracking for PV system. In: Proceedings of IEEE 2002 28th Annual Conference of the Industrial Electronics Society (IECON 02), Sevilla, Spain, pp. 3280–3284.

Xiao, W., Dunford, W.G., 2004. A modified adaptive hill climbing MPPT method for photovoltaic power systems. In: Proceedings of 35th Annual IEEE Power Electronics. Specialists Conference, Aachen, Germany. pp. 1957–1963.

Yu, G.J., Jung, Y.S., Choi, J.Y., Kim, G.S., 2004. A novel two-mode MPPT control algorithm based on comparative study of existing algorithms. Sol. Energy 76, 455–463.